Applied Physics Letters

RESEARCH ARTICLE | JULY 24 2025

Structure of the very first atomic layer of Ga oxide on GaN at GaN oxidation front

Emi Kano ; Shuto Hattori ; Kenji Shiraishi ; Atsushi Oshiyama ; Takahide Umeda ; Tetsuo Narita ; Tetsu Kachi ; Nobuyuki Ikarashi

Appl. Phys. Lett. 127, 032112 (2025)
https://doi.org/10.1063/5.0274521

AIP Publishing

Applied Physics Letters ARTICLE pubs.aip.org/aip/apl

Structure of the very first atomic layer of Ga oxide on GaN at GaN oxidation front

Cite as: Appl. Phys. Lett. **127**, 032112 (2025); doi: 10.1063/5.0274521
Submitted: 7 April 2025 · Accepted: 4 July 2025 ·
Published Online: 24 July 2025

Emi Kano,[1] Shuto Hattori,[2] Kenji Shiraishi,[1,2] Atsushi Oshiyama,[1] Takahide Umeda,[3] Tetsuo Narita,[4] Tetsu Kachi,[1] and Nobuyuki Ikarashi[1,a)]

AFFILIATIONS

[1]Institute of Materials and Systems for Sustainability, Nagoya University, Nagoya, Aichi 464-8601, Japan
[2]Graduate School of Engineering, Nagoya University, Nagoya, Aichi 464-8603, Japan
[3]Institute of Applied Physics, University of Tsukuba, Tsukuba 305-8573, Japan
[4]Toyota Central R&D Labs., Inc., Nagakute, Aichi 480-1192, Japan

[a)]Author to whom correspondence should be addressed: ikarashi@imass.nagoya-u.ac.jp

ABSTRACT

The atomic structure of the GaN oxidation front formed by oxide deposition followed by annealing was analyzed using atomic-resolution transmission electron microscopy and first-principles calculations. The oxidation front displays a terrace-step morphology, with atomically flat terraces and GaN monolayer steps. Our analysis clearly demonstrates that oxidation produces an epitaxial Ga oxide layer atop GaN. Furthermore, interfacial Ga atoms are situated near stacking fault positions of the underlying GaN lattice, forming dislocation-like structures at interface steps. These structural imperfections are expected to introduce states within the bandgap, offering insights into strategies for improving the electronic properties of GaN-based metal–oxide–semiconductor interfaces.

Metal–oxide–semiconductor field-effect transistors (MOSFETs) are foundational to modern electronics due to their high efficiency, fast switching speeds, and low power consumption. A critical factor in MOSFET performance is the nature of the oxide/semiconductor interface, as electrically active defects at or near this interface degrade key device characteristics, including carrier transport and threshold voltage stability.[1,2] In silicon-based technology, the structure and oxidation dynamics of the SiO_2/Si interface have been extensively studied both theoretically and experimentally, revealing atomic-scale insights into interfacial structure and defect formation.[3–6]

In the development of GaN-based MOSFETs, significant attention has been directed toward electrically active states—commonly referred to as *interface states*—at or near the oxide/GaN (0001) interface, which critically influence channel mobility and threshold voltage stability. These interface states have been detected within the fundamental bandgap at MOS interfaces formed with various oxides,[7,8] including Ga_2O_3,[9,10] Al_2O_3,[11–13] SiO_2,[14–17] and $Al_xSi_{1-x}O$ (AlSiO).[18–20] Recent studies indicate that interface states near the conduction band edge can be significantly suppressed through optimized fabrication conditions.[12,15,16] However, states near the valence band edge remain problematic,[8] and their origin—whether stemming from intrinsic defects, impurities, or their complexes—remains poorly understood. Structural defects at the oxide/GaN interface and oxygen vacancies within the oxide layer have been proposed as primary sources of these states,[7,8,12,17,21,22] and Mg doping has been shown to passivate such defects.[23]

In a standard GaN-MOS fabrication process, an oxide layer is deposited on the GaN surface under an oxidizing atmosphere and subsequently annealed in O_2 or N_2 ambient at temperatures ranging from 300 to 1050 °C—a process referred to as post-deposition annealing (PDA). During this treatment, the GaN surface undergoes inevitable oxidation, forming a nanometer-thick Ga oxide interlayer between the deposited oxide and GaN substrate.[16,19] To address interface state formation, it is essential to first elucidate the atomic-scale structure of the GaN oxidation front. Our previous theoretical work suggested that a crystalline Ga oxide atomic layer can form on the GaN surface during oxidation.[24] Experimental studies have reported on the Ga oxide/GaN structure[7,25,26] and an atomically abrupt interface has been observed for GaN (0001) surfaces oxidized below 800 °C.[27] Nonetheless, the precise atomic configuration of this interface has not yet been clarified.

Here, we report the atomic structure of the oxidation front of GaN (0001) formed during a standard GaN-MOS fabrication process,

as revealed by atomic-resolution transmission electron microscopy (TEM). Our experimental observations, in conjunction with first-principles calculations on the Ga oxide/GaN interface,[24] clearly demonstrate the formation of an epitaxial Ga oxide atomic layer directly atop the GaN substrate. The Ga atoms at the interface exhibit preferential octahedral coordination with six oxygen atoms. Furthermore, we provide direct evidence that the Ga oxide/GaN interface is composed of atomically flat terraces interspersed with monolayer-height steps corresponding to GaN (0001) lattice spacing. The Ga–O coordination at these steps induces dislocation-like structures, which may act as intrinsic defects contributing to interface states.

The analyzed Ga oxide/GaN interface was formed within an AlSiO/GaN structure fabricated via a standard GaN-MOS process. The AlSiO layer was deposited using plasma-enhanced atomic layer deposition (PEALD) at 250 °C onto a free-standing GaN substrate. The substrate surface comprised a 1-μm-thick Mg-doped p-type GaN layer (Mg concentration: 1×10^{17} cm^{-3}) grown by metal-organic vapor phase epitaxy (MOVPE). Prior to AlSiO deposition, the GaN surface was chemically cleaned using sulfuric and hydrochloric acid solutions, followed by treatment with diluted hydrofluoric acid. The deposited AlSiO film was 40 nm thick with a Si/(Si + Al) atomic ratio of 21%. PDA was conducted at 700 °C for 60 min in an N_2 atmosphere at 400 MPa.[28] Notably, high-pressure N_2 annealing is known to reduce interface state density more effectively than annealing at atmospheric pressure. The electrical characteristics of MOSFETs fabricated using similar conditions are detailed in our previous report (sample #1).[19]

Atomic-resolution imaging was conducted using high-angle annular dark-field scanning TEM (HAADF-STEM) at an acceleration voltage of 200 kV, with a spherical aberration coefficient below 1 μm. The inner and outer detector angles were 50 and 150 mrad, respectively. Cross-sectional TEM specimens were prepared by mechanical thinning followed by Ar-ion milling, including a final low-energy (500 eV) Ar-ion treatment to minimize ion-beam-induced artifacts. Specimen thickness ranged from 10 to 15 nm.[29,30]

HAADF-STEM image simulations were performed using a multislice algorithm, based on atomic models generated from first-principles calculations. The amorphous Ga oxide layer on GaN was modeled via a melt-quench molecular dynamics (MD) approach, followed by structural optimization within the generalized gradient approximation.[31] Four structurally distinct amorphous models (A–D) were created by varying MD conditions,[24] reflecting the structural variability of Ga oxide under different oxidation environments. Nonetheless, in all models, most of the interfacial Ga atom forms bonds with six neighboring O atoms in a nearly octahedral configuration, a common feature across the simulated Ga oxide/GaN interfaces.

A representative cross-sectional HAADF-STEM image is shown in Fig. 1. The incident beam direction is $\langle 11\bar{2}0 \rangle$. In the lower region, Ga atoms appear as bright spots. Under the current imaging conditions, N and O atoms are not visible. The upper dark region corresponds to the amorphous AlSiO layer. The step between atomically flat terraces on the left and right sides represents the height of a GaN monolayer. The lateral width of flat regions is typically less than 10 nm. Across all observations, the oxide/GaN interface consistently exhibits a terrace-step morphology comprising atomically flat terraces and monolayer-height steps.

To quantitatively evaluate lattice spacing at the interface, we analyzed the (0001) Ga lattice planes in atomically flat regions. Figure 2(a) shows a magnified HAADF-STEM image, and Fig. 2(b) presents the corresponding image intensity profile in the depth (c-axis) direction, averaged over 2 nm parallel to the interface. Intensity peaks denote Ga lattice planes. Gaussian fits to these peaks [Fig. 2(c)] were used to determine Ga-plane positions, from which lattice spacings were extracted [Fig. 2(d)]. Spacings S_1–S_6 are nearly constant, representing the bulk GaN (0001) lattice with an average value of 0.26 nm.[24,32] Minor fluctuations are attributed to experimental noise. Notably, spacing S_0—between planes 0 and 1—measures 0.29 nm, ~12% larger than S_1–S_6. Across ten measurements, S_0 averaged 0.29 ± 0.01 nm. The regular contrast of bright spots in Ga-plane 0 indicates a periodic atomic arrangement of Ga atoms, while the enlarged S_0 suggests a distinct structural configuration from bulk GaN.

To interpret this anomalous expansion, HAADF-STEM image simulations were performed using the theoretical Ga oxide/GaN structures from a previous study.[24] Figure 3(a) displays a simulated image for model A, with its intensity profile shown in Fig. 3(b). The triangles along the horizontal axis indicate the averaged positions of Ga atoms in the $\langle 0001 \rangle$ direction for each atomic plane, marking the locations of corresponding Ga atomic layers. Image simulations of all interface structures confirm that the peak positions in the intensity profiles align with the Ga atomic planes, verifying that the spacing between intensity peaks in the experimental images directly corresponds to Ga-plane spacing.

Table I presents the values of spacing S_0 and the average of S_1–S_5 for both theoretical models and experimental measurements. In all theoretical structures, S_0 ranges from 0.29 to 0.30 nm and exceeds the average of S_1–S_5 by approximately 12%–15%. This expansion arises from the insertion of O atoms between Ga planes 0 and 1, which stabilizes the structure through the formation of a Ga–O–Ga bond network. This structural feature observed in theoretical models is consistent with the experimental images shown in Fig. 2. Therefore, we conclude that the experimentally observed expansion of the spacing

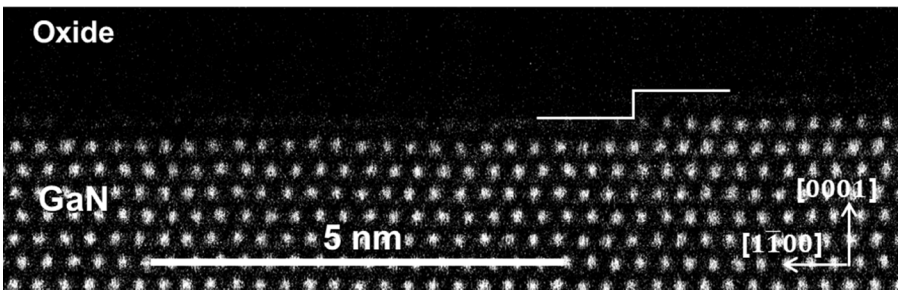

FIG. 1. HAADF-STEM cross-sectional image of oxide/GaN interface. Bright dots show Ga atomic positions. GaN monolayer interface step is indicated in the figure. Terrace-step structure was observed at interface.

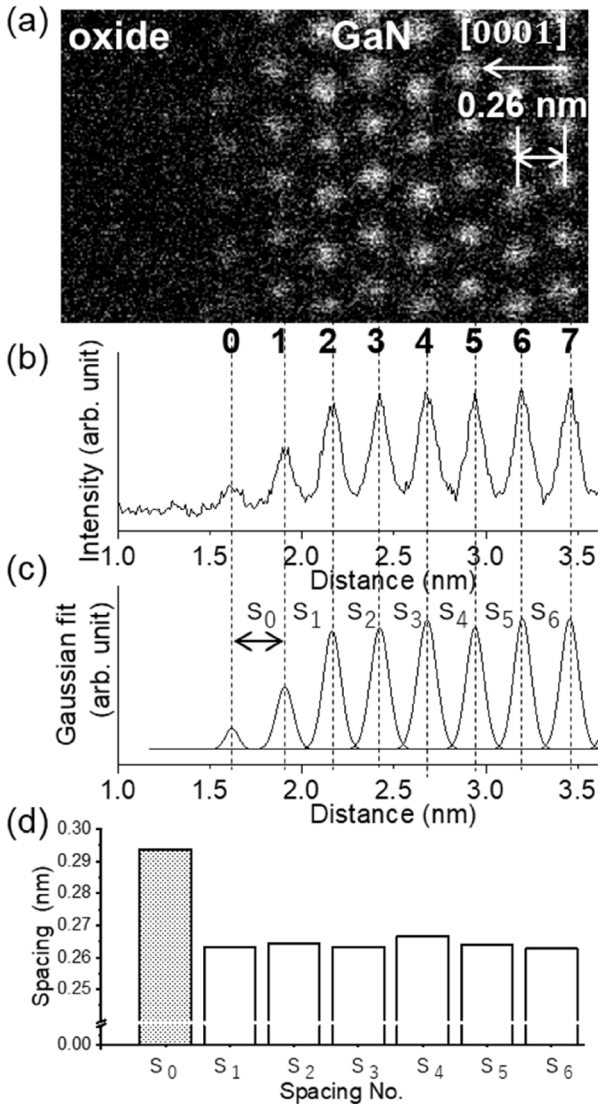

FIG. 2. (a) Close up of interface. Ga atomic planes are denoted from 0 to 7. (b) Image intensity distribution in (a). Horizontal axis in (b) is shown at same scale as micrograph. (c) Gaussian curves fitted to peaks in (b). Centers of Gaussian curves are used as positions of peaks of image intensity. Spacing between peaks 0 and 1 is denoted as S_0. (d) Lattice spacings in (c). S_0 is significantly larger than S_1–S_6.

between Ga planes 0 and 1 results from the presence of interstitial O atoms.

Further HAADF-STEM analysis reveals that Ga atoms in the interfacial Ga oxide layer occupy stacking fault positions relative to the underlying GaN lattice. This displacement arises from the nearly octahedral Ga–O coordination at the interface. Figure 4 illustrates a distinct atomically flat interface region, corroborating the structural features described above. Wurtzite GaN exhibits ABAB stacking along the ⟨0001⟩ direction, as illustrated in Fig. 4; the Ga atoms in Ga planes 1–7 occupy the A or B stacking positions. In contrast, the Ga atoms in Ga-plane 0 deviate from these positions and instead align with the

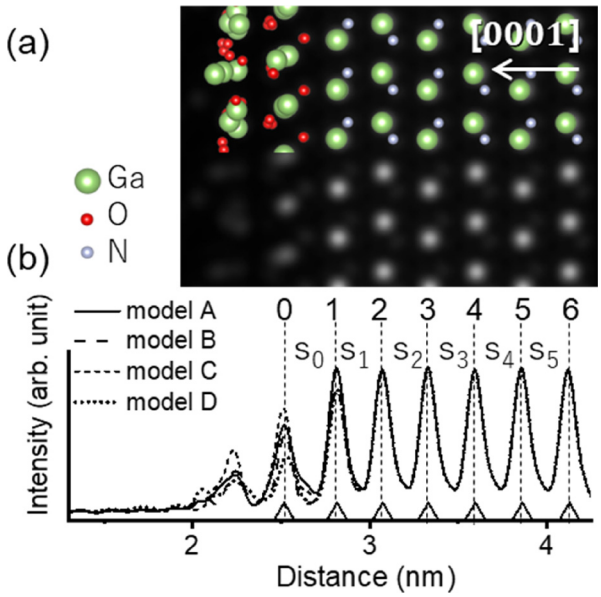

FIG. 3. (a) Simulated HAADF-STEM image of theoretical structure. Model A is used for simulation, and atomic positions in model are indicated by balls. (b) Image intensity distributions in simulated images of all theoretical structures. Triangles on horizontal axis show Ga-plane positions of model A.

TABLE I. Lattice spacings in nanometer.

		S_0	S_1 and below
Experiment		0.29	0.26
Model	A	0.30	0.26
	B	0.30	0.26
	C	0.29	0.26
	D	0.29	0.26

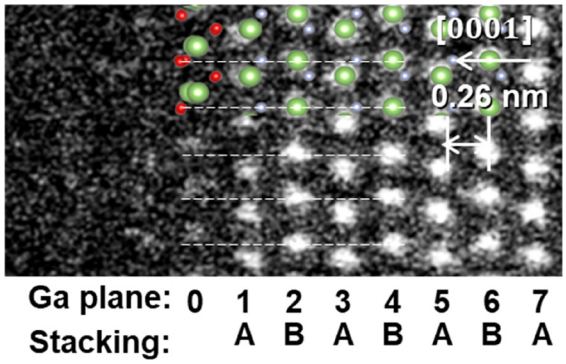

FIG. 4. Stacking fault between Ga oxide and GaN. Ga planes 1–6 show ABAB stacking sequence of wurtzite GaN. Dashed lines indicate B stacking position. Ga atoms of Ga-plane 0 are not at A or B stacking position. Schematic shows atomic positions in model C, where all interfacial Ga atoms are close to stacking fault position. Observed stacking positions of Ga atoms in Ga-plane 0 and in model C match.

configuration denoted as model C[24] (depicted by the overlaid atomic model), in which all interfacial Ga atoms are octahedrally coordinated with six O atoms and are located near the stacking fault position. Our theoretical calculations show that interfacial Ga atoms with octahedral Ga–O coordination do not occupy A or B sites but instead lie close to the stacking fault position in wurtzite GaN, as shown in Figs. 4(a) and 4(b) of a previous study.[24] The positions of interfacial Ga atoms in all theoretically derived structures are provided in the supplementary material. Notably, in these structures, 75% of the interface Ga atoms are coordinated with six O atoms. Therefore, the atomic arrangement observed in Fig. 4 provides experimental evidence for the theoretically predicted formation of a stacking fault structure at the interface. In contrast, Fig. 2(a) shows that the Ga atoms in Ga-plane 0 occupy the standard wurtzite stacking position. These findings collectively indicate that interfacial Ga atoms adopt stacking fault positions in certain regions of the interface, while in others they retain the wurtzite configuration.

The presence of a stacking fault structure between the Ga oxide layer and the GaN surface suggests that the interface step induces a dislocation-like defect. Specifically, in a Ga (0001) plane containing an interface step, one side of the step comprises GaN with wurtzite stacking and the other, Ga oxide. When Ga oxide adopts a stacking fault position, the step acts as a boundary between faulted and unfaulted (wurtzite) Ga atomic planes, resulting in a dislocation-like structure characterized by a Burgers vector $\boldsymbol{b} = 1/3\langle 1\bar{1}00\rangle$. Such structural defects at the interface are likely to produce dangling bonds that introduce electronic states within the bandgap, acting as hole or electron traps.[7,8] Our prior theoretical work has demonstrated that an atomically flat Ga oxide/GaN interface does not generate such defects.[24] However, the present results show that the Ga oxide/GaN interface comprises a terrace-step structure, where atomically flat terraces are interspersed with GaN monolayer steps that form dislocation-like structures. These steps are therefore expected to introduce structural imperfections that give rise to interface states. Prior studies have shown that the density of interface states and the structure of the Ga oxide/GaN interface—such as the thickness of the interfacial Ga oxide layer—vary with device fabrication conditions.[33] This implies that the atomic structure of the interface influences interface state density, which is consistent with our findings. Nevertheless, the precise mechanism by which interface structure affects interface state density remains unresolved. Our results suggest that controlling the formation of interfacial steps during device processing could be a viable strategy for reducing interface state density and enhancing device performance.

In the current experiment, image intensity peaks closer to the interface were generally lower, as observed in Fig. 2. This can be partially attributed to the geometry of the TEM specimens, which taper in thickness from the GaN substrate toward the AlSiO side, resulting in reduced image intensity near the AlSiO/GaN interface. Specifically, the peak intensity of Ga-plane 0 in the experimental image [Fig. 2(b)] was lower than that in the simulated HAADF-STEM image [Fig. 3(b)], likely due to experimental noise obscuring weak signals.

In summary, we have analyzed the atomic structure of the GaN oxidation front formed during a standard MOS fabrication process using atomic-resolution TEM combined with first-principles calculations. The oxidation front exhibits a terrace-step morphology, comprising an atomically flat Ga oxide/GaN interface and GaN monolayer steps. At the flat interface, an epitaxial Ga oxide layer is observed directly above GaN, and the interfacial Ga atoms locally occupy positions near the stacking fault of wurtzite GaN, suggesting that interface steps give rise to dislocation-like defects. These interfacial steps are thus likely to induce structural imperfections that lead to interface states.

See the supplementary material for details on the stacking positions of the Ga atoms of Ga-plane 0 (the interface Ga atomic plane of the Ga oxide atomic layer).

This work was partly supported by the MEXT Program for Creation of Innovative Core Technology for Power Electronics Grant No. JPJ009777 and JSPS KAKENHI Grant No. 20H00340.

AUTHOR DECLARATIONS

Conflict of Interest

The authors have no conflicts to disclose.

Author Contributions

Emi Kano: Conceptualization (equal); Data curation (equal); Formal analysis (equal); Investigation (equal); Methodology (equal); Validation (equal); Visualization (equal); Writing – original draft (equal); Writing – review & editing (equal). **Shuto Hattori:** Data curation (equal); Formal analysis (equal); Investigation (equal); Methodology (equal); Writing – original draft (equal); Writing – review & editing (equal). **Kenji Shiraishi:** Conceptualization (equal); Investigation (equal); Methodology (equal); Supervision (equal); Validation (equal); Writing – review & editing (equal). **Atsushi Oshiyama:** Conceptualization (equal); Investigation (equal); Methodology (equal); Supervision (equal); Validation (equal); Writing – review & editing (equal). **Takahide Umeda:** Conceptualization (equal); Investigation (equal); Methodology (equal); Writing – review & editing (equal). **Tetsuo Narita:** Conceptualization (equal); Investigation (equal); Methodology (equal); Writing – review & editing (equal). **Tetsu Kachi:** Conceptualization (equal); Investigation (equal); Methodology (equal); Writing – review & editing (equal). **Nobuyuki Ikarashi:** Conceptualization (equal); Data curation (equal); Funding acquisition (equal); Investigation (equal); Methodology (equal); Project administration (equal); Supervision (equal); Validation (equal); Writing – review & editing (equal).

DATA AVAILABILITY

The data that supports the findings of this study are available within the article and its supplementary material.

REFERENCES

[1]D. K. Schroder and J. A. Babcock, J. Appl. Phys. **94**, 1–18 (2003).
[2]Y. Taur and T. H. Ning, *Fundamentals of Modern VLSI Devices* (Cambridge University Press, 2021).
[3]P. E. Batson, Nature **366**, 727 (1993).
[4]F. M. Ross, J. M. Gibson, and R. D. Twesten, Surf. Sci. **310**, 243 (1994).
[5]H. Kageshima and K. Shiraishi, Phys. Rev. Lett. **81**, 5936 (1998).
[6]N. Ikarashi, K. Watanabe, and Y. Miyamoto, Phys. Rev. B **62**, 15989 (2000).
[7]J. T. Asubar, Z. Yatabe, D. Gregusova, and T. Hashizume, J. Appl. Phys. **129**, 121102 (2021).
[8]T. Narita, K. Ito, H. Iguchi, D. Kikuta, M. Kanechika, K. Tomita, S. Iwasaki, K. Kataoka, E. Kano, N. Ikarashi, M. Horita, J. Suda, and T. Kachi, Jpn. J. Appl. Phys., Part 1 **63**, 120801 (2024).

[9]H. Kim, S.-J. Park, and H. Hwang, J. Vac. Sci. Technol. B **19**, 579 (2001).
[10]Y. Nakano and T. Jimbo, Appl. Phys. Lett. **82**, 218 (2003).
[11]M. Ťapajna, M. Jurkovič, L. Válik, Š. Haščík, D. Gregušová, F. Brunner, E. M. Cho, and J. Kuzmík, Appl. Phys. Lett. **102**, 243509 (2013).
[12]T. Hashizume, S. Kaneki, T. Oyobiki, Y. Ando, S. Sasaki, and K. Nishiguchi, Appl. Phys. Express **11**, 124102 (2018).
[13]Y. Irokawa, T. Nabatame, K. Yuge, A. Uedono, A. Ohi, N. Ikeda, and Y. Koide, AIP Adv. **9**, 085319 (2019).
[14]E. Al Alam, I. Cortés, M. P. Besland, A. Goullet, L. Lajaunie, P. Regreny, Y. Cordier, J. Brault, A. Cazarré, K. Isoird, G. Sarrabayrouse, and F. Morancho, J. Appl. Phys. **109**, 084511 (2011).
[15]T. Yamada, D. Terashima, M. Nozaki, H. Yamada, T. Takahashi, M. Shimizu, A. Yoshigoe, T. Hosoi, T. Shimura, and H. Watanabe, Jpn. J. Appl. Phys., Part 1 **58**, SCCD06 (2019).
[16]K. Onishi, T. Kobayashi, H. Mizobata, M. Nozaki, A. Yoshigoe, T. Shimura, and H. Watanabe, Jpn. J. Appl. Phys., Part 1 **62**, 050903 (2023).
[17]K. Tomigahara, M. Hara, M. Nozaki, T. Kobayashi, and H. Watanabe, Appl. Phys. Express **17**, 081002 (2024).
[18]D. Kikuta, K. Ito, T. Narita, and T. Kachi, Appl. Phys. Express **13**, 026504 (2020).
[19]K. Ito, S. Iwasaki, K. Tomita, E. Kano, N. Ikarashi, K. Kataoka, D. Kikuta, and T. Narita, Appl. Phys. Express **16**, 074002 (2023).
[20]H. Iguchi, T. Narita, K. Ito, S. Iwasaki, E. Kano, N. Ikarashi, K. Tomita, and D. Kikuta, Appl. Phys. Lett. **125**, 022104 (2024).
[21]M. Choi, J. L. Lyons, A. Janotti, and C. G. Van de Walle, Phys. Status Solidi B **250**, 787 (2013).
[22]S. Hattori, A. Oshiyama, and K. Shiraishi, Appl. Phys. Lett. **125**, 161601 (2024).
[23]H. Mizobata, M. Nozaki, T. Kobayashi, T. Shimura, and H. Watanabe, Appl. Phys. Express **16**, 105501 (2023).
[24]S. Hattori, A. Oshiyama, and K. Shiraishi, J. Appl. Phys. **135**, 175303 (2024).
[25]K. Mitsuishi, K. Kimoto, Y. Irokawa, T. Suzuki, K. Yuge, T. Nabatame, S. Takashima, K. Ueno, M. Edo, K. Nakagawa, and Y. Koide, Jpn. J. Appl. Phys., Part 1 **56**, 110312 (2017).
[26]Y. Irokawa, K. Mitsuishi, T. Nabatame, K. Kimoto, and Y. Koide, Jpn. J. Appl. Phys., Part 1 **57**, 118003 (2018).
[27]T. Yamada, J. Ito, R. Asahara, K. Watanabe, M. Nozaki, S. Nakazawa, Y. Anda, M. Ishida, T. Ueda, A. Yoshigoe, T. Hosoi, T. Shimura, and H. Watanabe, J. Appl. Phys. **121**, 035303 (2017).
[28]M. Kanechika, T. Hirata, T. Tokozumi, T. Kachi, and J. Suda, Appl. Phys. Express **17**, 016502 (2024).
[29]K. Tsuda and M. Tanaka, Acta Cryst. **55**, 939 (1999).
[30]T. Nagase, K. Chokawa, E. Kano, K. Fukuta, T. Sasaki, S. Fujikawa, M. Takahashi, K. Shiraishi, A. Oshiyama, T. Araki, and N. Ikarashi, J. Appl. Phys. **137**, 055702 (2025).
[31]J. P. Perdew, K. Burke, and M. Ernzerhof, Phys. Rev. Lett. **77**, 3865 (1996).
[32]H. Schulz and K. H. Thiemann, Solid State Commun. **23**, 815 (1977).
[33]T. Yamada, K. Watanabe, M. Nozaki, H. Yamada, T. Takahashi, M. Shimizu, A. Yoshigoe, T. Hosoi, T. Shimura, and H. Watanabe, Appl. Phys. Express **11**, 015701 (2018).